Saudi Journal of Biological Sciences 29 (2022) 1134–1146

Contents lists available at ScienceDirect

Saudi Journal of Biological Sciences

journal homepage: www.sciencedirect.com

Original article

Fabrication and characterization of noble crystalline silver nanoparticles from *Pimenta dioica* leave extract and analysis of chemical constituents for larvicidal applications

Dinesh Kumar, Pawan Kumar, Kumar Vikram, Himmat Singh *

ICMR-National Institute of Malaria Research, Dwarka, New Delhi 110077, India

ARTICLE INFO

Article history:
Received 11 August 2021
Revised 3 September 2021
Accepted 13 September 2021
Available online 20 September 2021

Keyword:
Fourier transform infrared spectroscopy
Gas chromatography–mass spectrometry
Liquid chromatography–mass spectrometry
Vector borne

ABSTRACT

The current works report the bio-efficacy of *Pimenta dioica* leaf derived silver nanoparticles (Pd@AgNPs) and leaf extract obtained trough different solvents against the larvae of malaria, filarial and dengue vectors. Synthesis of silver nanoparticles (AgNPs) was done by adding 10 ml of *P. dioica* leaf extract into 90 ml of 1 mM silver nitrate solution, a slow colour change was observed depicting the formation of AgNPs. Further, Pd@AgNPs was confirmed through Ultraviolet–visible spectroscopy which exhibited characteristic absorption peak at 422 nm wavelength. X-ray diffraction and selected area electron diffraction analysis confirmed monodispersed and crystalline nature of Pd@AgNPs with 32 nm an average size. Scanning electron microscopy and transmission electron microscopy showed the most of Pd@AgNPs were spherical and triangular in shape and energy-dispersive X-ray spectroscopy revealed silver elemental nature of nanoparticles. Zeta potential of Pd@AgNPs is highly negative which confirmed its stable nature. Pd@AgNPs showed prominent absorption peaks at 1015, 1047, 1243, 1634, 2347, 2373, 2697 and 3840 cm^{-1} which are corresponding to following compounds polysaccharides, carboxylic acids, water, alcohols, esters, ethers, amines, amides and phenol, respectively as reported by Fourier-transform infrared spectroscopy analysis. Gas chromatography–mass spectrometry and Liquid chromatography–mass spectrometry analysis revealed 39 and 70 compounds, respectively, which might be contributed for bio-reduction, capping, stabilization and larvicidal behavior of AgNPs. A comparable lethality (LC_{50} and LC_{90}) was observed in case of Pd@AgNPs over leaf extract alone. The potential larvicidal activity of Pd@AgNPs was observed against the larvae of *Aedes aegypti*,($LC_{50,}$ 2.605; $LC_{90,}$ 5.084 ppm) *Anopheles stephensi* ($LC_{50,}$ 3.269; $LC_{90,}$ 7.790 ppm) and *Culex quinquefasciatus* ($LC_{50,}$ 5.373; $LC_{90,}$ 14.738 ppm without affecting non-targeted organism, *Mesocyclops thermocyclopoides* after 72 hr of exposure. This study entails green chemistry behind synthesis of AgNPs which offers effective technique for mosquito control and other therapeutic applications.

1. Introduction

Mosquitoes are the primary agent for transmitting vector-borne diseases and causing a nuisance in public. Among them, the most prevalent are malaria, filaria and dengue, which are spread through infected *Anopheles*, *Culex* and *Aedes* mosquitoes and have major health issues though out the world especially in tropical and subtropical regions (McKerr et al., 2015). Malaria causing one million deaths per year with around 2 billion people at risk (Féat et al., 2019). Around 50–100 million people with clinical severities in case of dengue infection were reported with approximately 20,000 deaths occur annually (Féat et al., 2019) and Japanese encephalitis accounts for 30,000–50,000 deaths each year globally (Khader et al., 2018). Recently physical and chemical approaches employed frequently to control such deadly vector borne diseases. Physical methods are temporary solutions for mosquito control which includes removal of the mosquito development site, mosquito nets and protective clothings, etc. Meanwhile, insecticides of synthetic origin such as temephos and pyrethroids are most

* Corresponding author at: Vector Biology Group, ICMR- National Institute of Malaria Research, Delhi 110077, India..
E-mail address: hspawar@rediffmail.com (H. Singh).

Peer review under responsibility of King Saud University.

Production and hosting by Elsevier

https://doi.org/10.1016/j.sjbs.2021.09.052
1319-562X/

effective but have major drawbacks like mosquito resistance and environmental issue. It has been reported that *Aedes aegypti* mosquito species showed resistance toward the temephos (larvicide) and pyrethroids (adulticides) insecticides in some regions of Malaysia (Ranson et al., 2010) and in India (Bharati and Saha, 2018). The resistance mechanism might be due to the high rate of insecticidal applications as a result of which metabolism and alteration of target sites of vector species occur (Kumar et al., 2020). Insecticides of synthetic origin also have additional drawbacks like toxicity in non-target organisms, emerging deterrence in mosquito and not environmentally sustainable (Benelli and Beier, 2017). Therefore, environmental friendly innovating alternative approaches are needed which should be cost-effective, reliable and can be used commercially for mosquito control. From the literature survey, it was observed that botanical extracts and their derived metabolites can be considered as a good source of larvicidal product and commercially feasible. Besides botanical blends have certain advantages such as environmentally sustainable, non-toxic to non-target organism, easily available, selective, biodegradable and less chance of resistance due to different modes of action and complex structure of molecules (Kumar et al., 2020). Plant based nanoformulation have a group of compounds which have different mode of action and complex molecular structure thereby reduce the chance or leave a little chance of getting resistance in mosquitoes towards such compounds (Ghosh et al., 2015). But herbal formulations have some issue related to stability and low persistence efficacy which can be resolved by nanoformulations. Besides this, the controlled release of mosquito insecticides through nanoencapsulation techniques extends the stability and efficacy for longer period of time. In recent trends, biologically synthesized nanoparticles (10–100 nm) exhibited strong larvicidal potential against different mosquito vector species. AgNPs derived from plant extract have several advantages including easy available, safe, non-toxic and minimum downstream processing steps and most effective against mosquito due to their smaller in size (Saini et al., 2019). Plant derived AgNPs synthesis is also energy efficient, time effective and less precursor needed for its synthesis (Irshad et al., 2021). Various reports have already been available associated with plant-derived AgNPs and their potential application against the larvae of different mosquito vectors such as *Annona glabra* (Amarasinghe et al., 2020), *Catharanthus roseus* (Pavunraj et al., 2020), *Cullen corylifolium* (Saini et al., 2019), *Elytraria acaulis* (Rangayasami et al., 2020), *Leonotis nepetifolia* (Manimegalai et al., 2020), *Rhazya stricta* (Alshehri et al., 2020) and *Ricinus communis* (Waris et al., 2020). *Cymbopogon nardus* derived essential oil is commercial available against the different mosquito vector in Europe and North America (Covell, 1940). Permethrin and Para-methane 3–8, diol were obtained from *Chrysanthemum cinerariifolium* and *Corymbia citriodora*, plant respectively have been reported for mosquitocidal and repellant activity against several species of mosquito (Maia and Moore, 2011, Islam et al., 2017). Formulations and extract of some plant species including *Azadirachta indica, Ocimum tenuiflorum, Chrysanthemum coccineum* and *Lantana camara* have been effectively used against vectors (Shukla et al. 2018). Plant-derived nanoparticles are a safer and greener approach and the *Pimenta dioica* can be considered as a potential larvicide source to resolve the issue related to resistance from chemical, biomagnifications or bioaccumulation of compounds. *Pimenta dioica* (family Myrtaceae) is an aromatic medicinal plant and commonly called Allspice and widely distributed in South America, Mexico and West Indies. It has a wide range of applications including natural pesticides, perfumes, biomedicine, food spices and antifungal (Irshad et al., 2021). The plant has various therapeutic properties such as antimicrobial, antioxidant, antiseptic, carminative, muscle relaxant, stimulant and menopause (Marzouk et al., 2007). Antimicrobial potential of *P. dioica* have already been reported towards different pathogens such as *Staphylococcus aureus, Acinetobacter baumannii, Escherichia coli* and antifungal potential towards *Candida albicans, Fusarium oxysporum Aspergillus niger, Penicillium brevicompactum and Abisidia corymbifera* (Zabka et al., 2009; Ismail et al., 2020). Gold nanoparticles of prepared using *P. dioica* have been reported for antibacterial activity against gram-positive and gram-negative bacteria such as *Staphylococcus aureus* and *Escherichia coli*, respectively (Fadaka et al., 2021). A significant anticancer activity of *P. dioica* derived iron oxide nanoparticles was previously reported against human colorectal cancer cells with less affect normal L929 (fibroblast) cells (Pillai et al., 2021). Taking into account the enormous medicinal potential of this plant, it was proposed to (i) *Pimenta dioica* leaf derived AgNPs synthesis (Pd@AgNPs), (ii) characterization employing SEM, TEM, UV–Vis spectroscopy, FT-IR, (iii) LC-MS and GC–MS analysis of plant extract in order to find out compounds involved in AgNPs bio-reduction and, (iv) larvicidal activity of leaf extract prepared in solvent and AgNPs against *Cx quinquefasciatus*, *An. stephensi*, *Ae. aegypti,* and *M. thermocyclopoides*.

2. Materials and methods

2.1. Preparation of Pimenta dioica leaf extract

Leave of *Pimenta dioica* were collected from the plant grown in Prakriti garden studio (latitude 28.63°N; longitude 77.22°E), Mandi, New Delhi and washed several times to remove the dust and impurities. Leave were air dried at room temperature for a weak and cut into small pieces and ground into coarse powder. Subsequently, powder was divided into several parts (10 g each) and was soaked in a conical flask containing 200 ml of double distilled water to obtain plant extract, separately. The extract was kept on incubator shaker with 130 rpm for 30 min with slightly boiling temperature in case of aqueous leaf extract. For solvent extract preparation, 10 g leaf powder was kept on incubator shaker in a 250 ml of weaker containing 200 ml of different solvents (methanol, chloroform, hexane, petroleum ether and acetone), individually, at 140 rpm for 72 hr at room temperature. The leaf extract was filtered through Whatman filter paper No.1 to remove residue and supernatant was concentrated and stored at 4 °C for larvicidal bioassays.

2.2. Preparation of Pimenta dioica fabricated silver nanoparticles

The synthesis of silver nanoparticles was done using green approach as previously adopted by Kumar et al. (2018a,b) after adding some modifications. Aliquots 10 ml of leaf extract of *Pimenta dioica* was added into a flask containing 90 ml of 1 mM of $AgNO_3$ with constant stirring for 20 min at 60 ± 3 °C of temperature. After the addition, the colour of the solution was changed slowly form pale yellowish to dark brown depicted the synthesis of silver nanoparticles. Further, centrifugation of solution was done at 10,000 rpm for 20 min, in order to find out the residue. Residue was collected, washed with double distilled water, concentrated and stored at 4 °C for characterizations and larvicidal application.

2.3. Characterization of Pimenta dioica mediated silver nanoparticles

The change in colour of the solution from yellow to dark brown was observed through naked eyes which indicate the bio-reduction silver nitrate to AgNPs. Further confirmation was done through UV–Vis spectrophotometer (Shimadzu 250 version 2.33) analysis and its wavelength range was 350 to 800 nm. Silver nanoparticles produced under standard conditions ($AgNO_3$: 1 mM; Temperature: 60 ± 3 °C; Time: 20 min) were centrifuged and pellet was collected

and supernatant discarded. Pellet was washed several times and converted into powder through freeze dried. 5 mg of the sample was subjected to XRD analysis through Philips Xpert pro-XRD System operated under following conditions current 40 mA with Cu ka radiation of 0.1541 nm; voltage, 40kV; step size, 0.02/h, 2θ range 20°–80°. Shape of developed nanoparticles was determined through Scanning electron microscope (STM-1000 SEM, Carl Zeiss EVO-40, München, Germany) at SAIF in All India Institute of Medical Sciences New Delhi, India. AgNPs powder was put on double conductive tape that was wrapped on sample holder at room temperature. For make sample conductive, sample was coated with thin layer of gold. Images were taken at 29 kV operation voltages. The images of Pd@AgNPs were taken using Transmission electron microscope (TEM; Tecnai G20 FEI, Oregon, USA) which was attached to EDX for elemental nature analysis. Dry powder of Pd@AgNPs sample was placed over the copper grid and images were captured at different magnification at RT. The operating was 50–300 kV in order to find out the shape and distribution of AgNPs. AgNPs (1 mg) suspended in Millipore (1 ml) water and were subjected to ultrasonication in order to complete dispersal for 10 min. Further stability of above AgNPs in the solution was confirmed through dynamic light scattering (Zetasizer Nano-ZEN3600, Malvern Instruments Pvt. Ltd., UK) which was working at RT. Potential function group contributed to creation and stabilization of AgNPs was classify in the plant extract through FT-IR (Perkin-Elmer 1600 series FT-IR spectrometer, Nujol, KBr disks) which was working on ATR mode. A drop was Pd@AgNPs (1 mg/ml; silver nanoparticles/methanol) which was properly mixed with potassium bromide and put on KBR plate and subject to FT-IR analysis. In order to find out chemical constituents present in plant extract it was subjected to Ultra GCMS-QP2010 PLUS GC–MS instrument coupled with auto sampler unit, AOC-20 s and auto-injector unit AOC-20i. Metabolites separation was done using RTX-5MS GC column having 30 m length, 0.25 mm diameter and 0.25 μm thick. One microliter sample dissolved in methanol was injected in auto sampler in the ratio of 1:10 in spilt mode with injection temperature 230 °C and column oven temperature 70 °C and helium used as a carrier gas with constant velocity of 40.3 cm/s. Mass spectrometry was run with following conditions: interface temperature 280 °C, 3.5 min solvent cut time and source temperature 230 °C. Mass scan range 40–650 *m*/*z* with total running time were 35.5 min. Xcalibur™ software fixed with GC–MS/MS system was used for analysis of mass spectra and chromatogram. Data acquired through GC–MS 2010QP-PLUS instruments was analyzed by post run software and more than 0.1% area peaks was picked and remained were discarded. Using RI markers (alkane mixture) automated RI calculations was done. NIST 05, NIST 08 and Wiley 08 mass spectral libraries was used for automated peak identifications having similarity index more than 75%. Both dimensions RI for GC and SI for MS were used for compounds identifications. LC-MS analysis of methanolic leaf extract was done using Synapt G2 associated with 2D nano ACQUITY System, Waters, USA and MALDI MS-ABI Sciex 5800 at AIRF JNU. Instrument was equipped with autosampler, column oven, binary pump, electrospray ionization source and in-line degasser. In order to identify possible bioactive compounds and peaks, LC-MS date were searched against the public data base with following parameters; Batch search, M+H and M+Na, positive mode with the accuracy of 10 ppm. XCMS/Metlin database was used for the identification of tentative metabolites in the *Pimenta dioica* plant extract.

2.4. Larvicidal activity of silver nanoparticles and Pimenta dioica leaf extract

Bio-efficacy of *Pimenta dioica* were evaluated against 3rd instar larvae of *Anopheles stephensi, Culex quinquefasciatus* and *Aedes aegypti* based on slight modification of WHO standard guidelines and procedure for larvicidal test method (WHO, 1988). Initial screening was done using selected plant extracts and AgNPs with different concentration ranging from 25 to 1000 ppm and 1 to 25 ppm, respectively. Stocks of the solution were prepared separately by dissolving 1 mg/ml of plant extract different solvent as well as AgNPs in dechlorinated water in 50 ml glass bottle. Using stocks solution, different dilutions of plant extract (20, 40, 60, 80, 100 and 120 ppm) and AgNPs (2.5, 5, 10, 20 and 25 ppm) were made individually, using double distilled water. Twenty five larvae of above said mosquito were taken in 249 ml of water having 1 ml of desired concentration of extracts or AgNPs. Individual solvent, 1 mM silver nitrate and tap water used as control and experiments were run in triplicate. Foreign particles entry was blocked by rapping the beaker using muslin cloth. After 24 hr of exposure, the larval mortality was recorded and food was provided. Experiments were run at room temperature and it was run till 72 hr. The mortality was corrected using Abbott's formula (Abbott, 1925).

$$\text{Corrected mortality} = \text{Obtained mortality (in treatment)} - \text{Obtained mortality (in control)}\ 100 - \text{Control (mortality)} \times 100$$

Non-targeted effect of AgNPs was done against the *Mesocyclops thermocyclopoides* which was obtained from Burari village and acclimatized in laboratory (National Institute of Malaria Research, New Delhi) for further experiments. *M. thermocyclopoides* larvae, 25 in number were placed in a beaker containing AgNPs solution and experiments were run in triplicate. Experiments were run along with a set of control and deceased larvae were recorded 24, 48 and 72 hr of exposure.

2.5. Recording of data

Mortality was assessed after 24, 48 and 72 hr exposure of plant extracts; the final morality was counted after 72 hr only after those larvae were counted as healthy in case they survived. Abbott's formula was applied if mortality in the control was found more than 5% and the test was discarded and repeated if control mortality was found more than 20%, the standard state of mortality was adopted followed WHO (1988) guidelines. A delayed mortality assay was adopted for the pant-based product. The experiments were done in triplicate with control without adding any plant extract. The standard state of mortality was adopted from WHO (1988) guidelines.

2.6. Statistical analysis

Log probit analysis was done in order to find out LC values (LC_{50}: lethal concentration causing 50% mortality in the population/LC_{90}: lethal concentration causing 90% mortality in the population) and few factor such as upper confidence limits (UCL), Chi-square values, lowers confidence limits (LCL), at 95% intervals (Finney, 1971). The obtained data were analyzed by regression analysis using the statistical program the SPSS software version 21, window 16.

3. Results

3.1. Synthesis and characterization of Pimenta dioica fabricated silver nanoparticles

AgNPs were prepared by mixing of leaf extract of *Pimenta dioica* into $AgNO_3$, a slow colour change from yellow to slight brown was seen, which depicted AgNPs synthesis. It was prominent after 20 min; which was the further visual confirmation of AgNPs synthesis (Fig. 1B). Further, Pd@AgNPs showed a prominent UV–Vis peak at 422 nm which proved the production of AgNPs (Fig. 1C). A similar UV–Vis spectrum reported after 6 weeks which confirmed the stable nature of AgNPs synthesis using *P. dioica* leaf extract (Fig. 1D). X-ray diffraction spectrum of AgNPs revealed four peak values at 38.24°, 44.61°, 64.48°, and 77.12° at 2θ corresponding to the (111), (200), (220), and (311) sets of lattice planes, respectively, which is related to crystalline nature with face centered cubic structures (Fig. 1E). XRD spectrum of also exhibited few smaller peaks due to existence of unidentified impurities in AgNPs powder. Pd@AgNPs was spherical and triangular shape with mean size of 25–60 nm as revealed through scanning electron microscope image (Fig. 1F). Transmission Electron Microscope (TEM) of Pd@AgNPs was triangular and spherical in shape with the average size of 20–40 nm (Fig. 2A&B). EDX spectrum of Pd@AgNPs depicted strong peak at 3.3 KeV due to SPR which confirmed the silver nature of AgNPs (Fig. 2C). EDX signal for Cu was also noted due to copper coating of the sample. The Selected area diffraction pattern (SAED) of Pd@AgNPs showed single-crystalline nature of particles which indicate their spot type pattern (Fig. 2D). The zeta potential of Pd@AgNPs was reported highly negative 21.4 mV (Fig. 2E). This high negative zeta potential of AgNPs inferred its good dispersion and stability by preventing its accumulation process. FT-IR spectrum of AgNPs showed absorption peaks at 1015, 1047, 1243, 1634, 2347, 2373, 2697 and 3840 cm^{-1} which represent following functional groups, C—O, N—H, C—F, C═C, H—C═O, C—H and O—H with corresponding compounds polysaccharides, alcohols, carboxylic acids, water, esters, ethers, 1°, 2° amines, amides, phenol, respectively (Table 1, Fig. 2F). *P. dioica* leaf extracts were analyzed through LC-MS and GC–MS instruments and reported several compounds which contributed in reduction, capping and stabilization of AgNPs and killing of mosquito vectors (Tables 2 and 3). Plant has several compounds which stabilized silver nanoparticles by preventing their over growth and agglomeration in colloidal suspension medium and act as capping agents. GC–MS revealed 39 compounds; among them major components are gamma-sitosterol, lupeol, alpha tocospiro B, neophytadiene, 4- allylphenol, eugenol and remaining in between of 1.5 and 0.16% (Figs. 3 and 4). LC-MS analysis revealed the presence of 70 compounds which have wide range of medicinal properties and might be participated for the reduction and capping of AgNPs.

3.2. Bio-efficacy of Pimenta dioica fabricated silver AgNPs and leaf extract

The bio-efficacy leaf extracts of *Pimenta dioica* and its derived AgNPs prepared in different solvents individually were assessed against *Aedes aegypti, Culex quinquefasciatus* and *Anopheles stephensi* larvae and the result were summarized in Table 4 and Figure 5 A & B. A strong larvicidal activity was reported in Pd@AgNPs over other leaf extract solvents towards *Ae. aegypti, An. stephensi* and *Cx. quinquefasciatus* having LC_{50} and LC_{90} value were 2.605, 3.269, 5.373, 5.084, 7.790 and 14.738 ppm, respectively, after 72 hr exposure. Of all the different solvents tried, *Pimenta dioica* leaf hexane extract was moderately effective and inducing cent percent mortality at minimal concentrations against *An. stephensi* (LC_{50}:15.01; LC_{90}:30.57 ppm), *Cx. quinquefasciatus* (LC_{50}:24.24; LC_{90}:43.28 ppm) and *Ae. aegypti* (LC_{50}:34.11; LC_{90}:62.65 ppm), respectively, after 72 hr of treatment. Whereas moderate larvicidal potential was reported in chloroform leaf extract *P. dioica* against 3rd instar larvae of *An. stephensi* (LC_{50}/LC_{90}; 20.72/39.99 ppm), *Cx. quinquefasciatus* (LC_{50}/LC_{90}; 26.24/38.53 ppm) and *Ae. aegypti* (LC_{50}/LC_{90}; 49.20/77.84 ppm) after 72 hr of exposure. Meanwhile, the methanol leaf extract of *P. dioica* reported for moderate activity with LC_{50} and LC_{90} values of 18.859, 43.84, 65.327, 38.50, 83.12 and 106.39 ppm against *An. stephensi*, *Cx. quinquefasciatus* and *Ae. aegypti*, respectively, after 72 hr of treatments. After 72 hr of exposure, a similar LC_{50} and LC_{90} values of 17.026, 58.99, 53.223, 41.424, 39.855, 73.698, 32.63, 86.77, 85.76, 63.37, 68.95 and 115.36 ppm were reported in case of acetone and petroleum ether leaf against *An. stephensi*, *Cx. quinquefasciatus* and *Ae. aegypti* mosquito vectors, respectively. LC_{50} and LC_{90} concentrations of Pd@AgNPs calculated against *An. stephensi*, *Cx. quinquefasciatus* and *Ae. aegypti* larvae were non-toxic against non –targeted organism *Mesocyclops thermocyclopoides* (data not shown) after 72 hr of treatment.

4. Discussion

4.1. Synthesis and characterization of Pimenta dioica fabricated silver nanoparticles

Nowadays, nanoparticles research is one of the most important areas in nanoscience due to the development of biocompatible, simple, eco-friendly, scalable, cost-effective techniques for nanoparticles synthesis and its wide range of applications. In this research work, a visual colour transition from yellow to dark brown predicted the development of AgNPs when *Pimenta dioica* leaf extract was mixed to $AgNO_3$. The colour change of the solution is directly related to Surface plasmon resonance (SPR) excitation of silver nano-material. AgNPs exhibited localized surface plasmon resonance when the surface electron of AgNPs interacts with electromagnetic radiation, generating localized surface plasmon resonance (LSPR) and produce scattered and extinction spectra in the UV–Visible range from 370 to 470 nm. However, the existence of biological agent can trigger aggregation-disaggregation incident which are directly related to change in LSPR band. This aggregation/disaggregation phenomenon responsible for alteration of λmax and intensity of SPR band which are directly related to colour change and blue/red shift of SPR band (Prosposito et al., 2020). The colour transition of AgNPs solution is directly associated with the synthesis of AgNPs as reported in *Annona glabra* by Amarasinghe et al. (2020). Synthesis of AgNPs evident from the notable transition from light yellowish brown to dark brown through mixing of $AgNO_3$ and *Blumea mollis* extract (Elumalai et al., 2020). Likewise, the synthesis of AgNPs using *Leonotis nepetifolia* leaf extract was confirmed by prominent peaks at 420 nm through UV–Vis spectra (Manimegalai et al., 2020). A similar absorption peak at 420 nm also observed in *Piper longum* derived AgNPs by Yadav et al. (2019). SPR band is responsible for size and shape, dielectric environment and composition of AgNPs. The variation of size of AgNPs directly correlated with width of SPR band (Petit et al., 1993). As the size of nanoparticles decreases, peaks in UV–Vis absorption spectra became broader (Kong and Jang, 2006). Till date, several studies have been done on the formation of AgNPs employing extracts of plants, but the exact mechanism behind AgNPs formation is still unknown (Kumar et al., 2020). As assumed in several studies, plant extract contains several compounds including phenolics, terpenoids, alkaloids, carbohydrates, proteins, flavonoids and nucleic acids that might be accountable for production of AgNPs employing plant extract (Chung et al., 2016). In

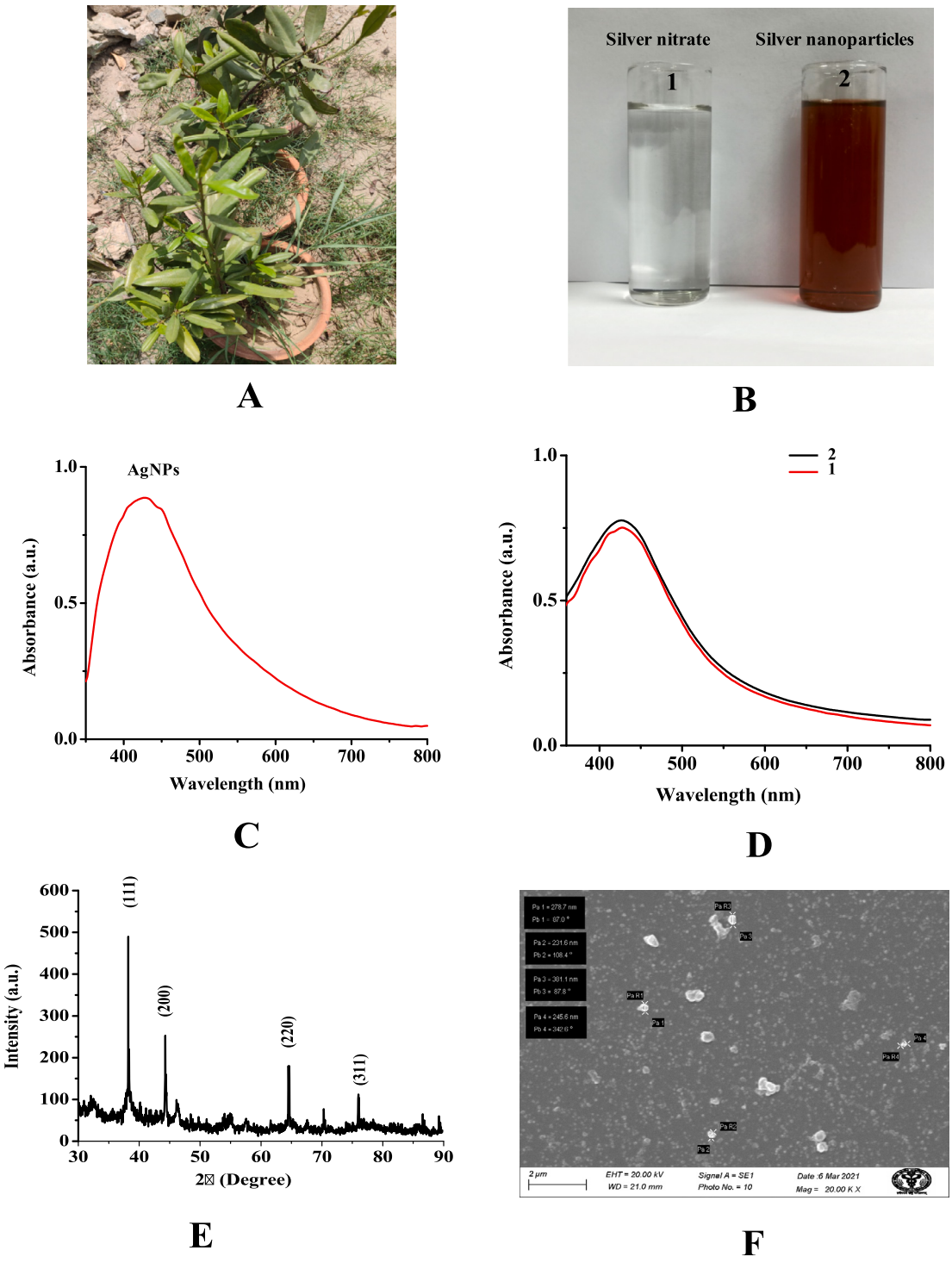

Fig. 1. (A) *In vivo* grown plant of *Pimenta dioica* in Prakriti garden studio, Mandi, New Delhi, India, (B) Silver nitrate without addition of *Pimenta dioica* leaf extract showed no color change (1) and after adding leaf extract showed visual color change from white to dark brown confirm silver nanoparticles synthesis (2), (C) Ultraviolet–visible spectrum of silver nanoparticles synthesized using *Pimenta dioica* leaf extract with 1 mM aqueous solution of silver nitrate showed characteristic absorption peak at 422 nm, (D) Ultraviolet–visible spectrum of silver nanoparticles synthesized using *Pimenta dioica* leaf extract after 20 min (1) and six weeks (2), (E) X-ray diffraction spectrum of silver nanoparticles synthesized employing aqueous leaf extract of *Pimenta dioica* showed their crystalline nature, (F) Scanning electron microscopy images of silver nanoparticles synthesized using aqueous leave extract *Pimenta dioica*.

Nothapodytes nimmoniana, the acceptance of an electron to Ag^{+} from phenolics compounds is pre-requirements for the synthesis of AgNPs through plant extract and silver nitrate (Mahendran and Kumari, 2016). In yet another study, NAD^{+} was the main constituents in the extract which are accountable for AgNPs production whereas some authors proposed carbonyl and hydroxyl groups were the important constituents participated in silver ion reduction (Chung et al., 2016). Pirtarighat et al. (2019) also observed that hydroxyl and carbonyl functional groups play a key role for the production of AgNPs in *Salvia spinosa*. Phenolics

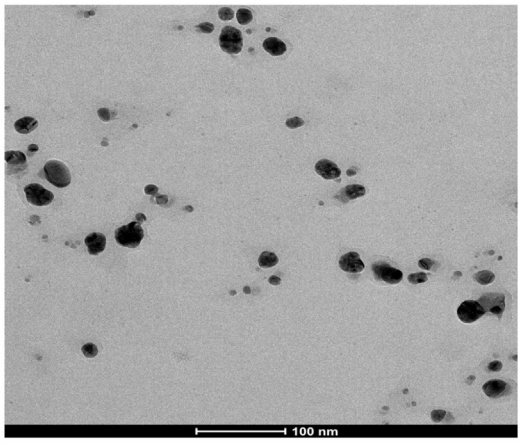

A

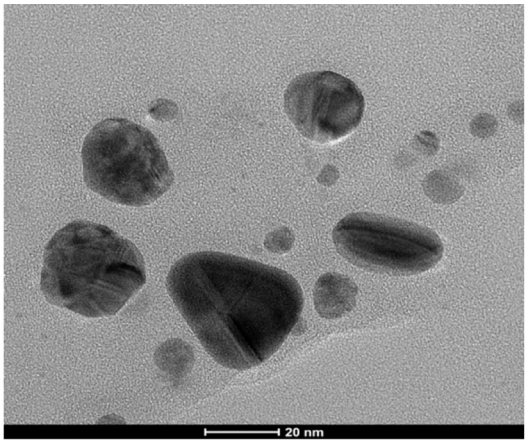

B

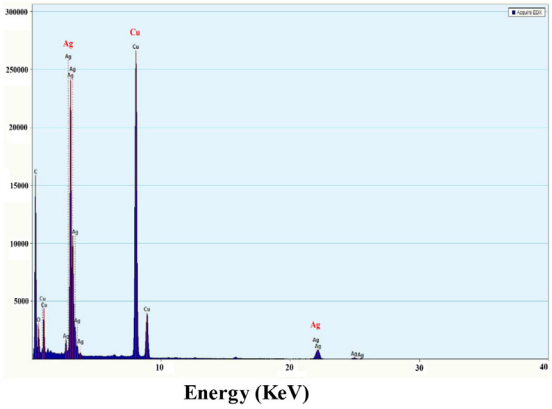

C

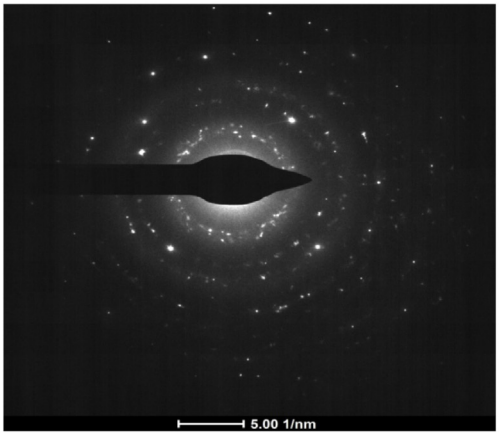

D

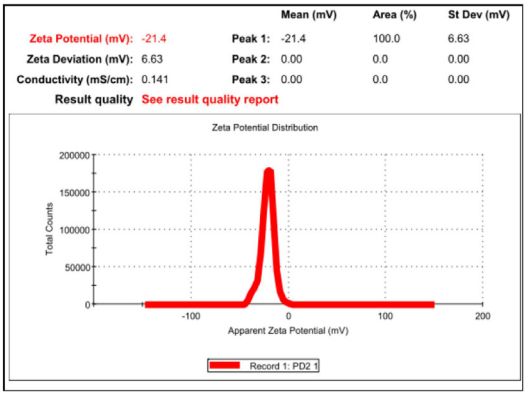

E

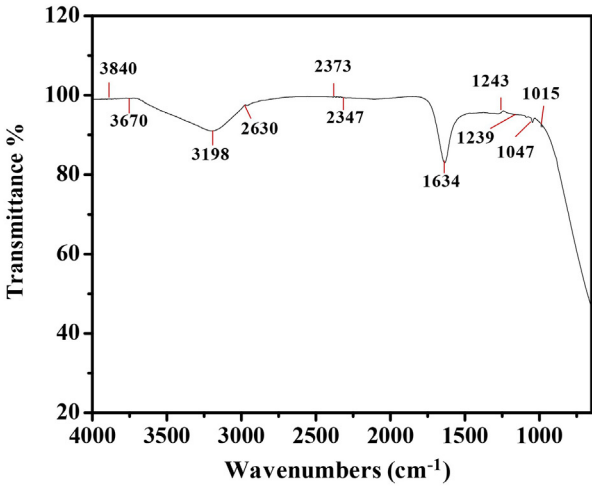

F

Fig. 2. (A & B) Transmission electron microscopy micrograph of silver nanoparticles derived from aqueous leaf extract *Pimenta dioica* showed spherical and triangular shape of AgNPs, (C) Energy-dispersive X-ray spectrum of synthesized AgNPs showing absorption band at 3 keV, (D) Selected area electron diffraction pattern of synthesized silver nanoparticles using aqueous leaf extract of *Pimenta dioica* showed their polycrystalline nature, (E) Zeta potential measurements of synthesized AgNPs using *Pimenta dioica*, (F) Fourier-transform infrared spectrum of synthesized silver nanoparticles derived aqueous leaf extract of *Pimenta dioica* showed occurrence of several functional groups.

Table 1
Fourier-transform infrared spectroscopy profile of silver nanoparticles prepared using leaf extract of *Pimenta dioica* and silver nitrate showed occurrence of several functional groups.

Frequency (CM^{-1})	Wave number (CM^{-1})	Functional groups	Class
1200–900	1015	O═C═O, C—O stretch	Polysaccharides
1075–1020	1047	C—O, N—H stretch	Vinylether, amide
1275–1200	1233	C—O stretch	Alkyl aryl ether
1320–1000	1239	C—O stretch	Alcohols, carboxylic acids, esters, ethers
1400–1000	1243	C—F, C—O stretch	Fluoro compound, alkyl aryl ether,
1670–1600	1634	C═C, N—H stretch	Alkene, conjugated alkene, amine
2400–2000	2347	N—H, C—O stretch	alcohols, carboxylic acids, esters, ethers, 1°, 2° amines, amides
2400–2000	2373	O═C═O stretch	Carbon dioxide
2830–2695	2697	H—C═O, C—H stretch	Aldehyde
3300–2500	3198	O—H stretch	Carboxylic acid, alcohol
3700–3100	3670	O—H Stretch	Water
4000–3000	3840	O—H stretch	Phenol, alcohol

(eugenol, 4-allylphenol, 2, 4-di-*tert*-butylphenol, theaflavin digallate and plantamajoside) and flavonoids (flavoxate, kaempferol and vitexin) and other compounds present in the *Pimenta dioica* leaf extract as revealed through GC and LC-MS analysis might be accountable for reduction, stabilization and capping of AgNPs in the present study also. XRD analysis of Pd@AgNPs along with four intense Bragg's reflection peaks proved the crystalline cubic character of the AgNPs. Rajput et al. (2020), while working on *Atropa acuminate* mediated AgNPs mentioned Bragg reflection values 38.06 (111), 44.22 (200), 64.24 (220) and 76.62 (311) at 2θ angle clearly indicates face-centered cubic structure with crystalline nature of AgNPs. In the case of *Leonotis nepetifolia* synthesized AgNPs, the following reflection peaks of 37.89, 45.91, 64.13, and 76.49 at 2θ angle which is directly related to (111), (200), (220), and (311) Bragg reflection values, respectively, which depicted the face-centered cubic nature (Manimegalai et al., 2020). The XRD analysis of *Andrographis serpyllifolia* leaf-derived AgNPs showed a number of peak values at 38.17, 44.27, 64.77 and 77.40 at 2θ angle which are correlated with crystalline nature and face-centered structure (Govindan et al., 2020). Few smaller peaks in form of impurities were also reported in XRD pattern of AgNPs. XRD spectrum *of Holarrhena antidysenterica* derived AgNPs also exhibited few similar peaks due to unidentified impurity (Kumar et al., 2018a,b). Rajakumar and Abdul Rahuman (2011) while working on AgNPs synthesized using *Eclipta prostrata* reported similar abnormal peaks in XRD spectrum. SEM and TEM images study of Pd@AgNPs revealed the triangular and spherical shaped nanoparticles within the range of 20–60 nm. Field emission electron micro-

Table 2
Chemical composition of the *Pimenta dioica* leaf extract obtained through Gas chromatography – mass spectrometry analysis.

Peak	R. Time	Area	Area%	Name
1	7.897	33,305,443	15.40	4-Allylphenol
2	9.246	112,123,100	51.85	Eugenol
3	11.186	1,315,569	0.61	2,4-Di-*tert*-butylphenol
4	12.175	1,112,099	0.51	Caryophyllene oxide
5	12.664	878,970	0.41	(1R,7S,E)-7-Isopropyl-4,10-dimethylenecyclodec-5-enol
6	12.880	1,455,264	0.67	Alpha-cadinol
7	13.552	650,078	0.30	2-Cyclohexen-1-one, 4-(3-hydroxybutyl)-3,5,5-trimethyl-
8	14.443	334,126	0.15	2(4 h)-benzofuranone, 5,6,7,7a-tetrahydro-6
9	14.560	765,045	0.35	(S,E)-4-Hydroxy-3,5,5-trimethyl-4-(3-oxobut-1-en-1-yl)cyc
10	14.835	4,355,257	2.01	Neophytadiene
11	15.089	2,613,405	1.21	2-hexadecen-1-ol, 3,7,11,15-tetramethyl
12	15.284	2,963,729	1.37	2-hexadecen-1-ol, 3,7,11,15-tetramethyl
13	15.751	936,758	0.43	Hexadecanoic acid, methyl ester
14	16.423	389,918	0.18	1-Nonadecene
15	16.887	528,656	0.24	Palmitic Acid, TMS derivative
16	17.386	694,470	0.32	9,12-Octadecadienoic acid (Z,Z)-, methyl ester
17	17.446	1,529,612	0.71	6-Octadecenoic acid, methyl ester, (Z)-
18	17.551	4,379,392	2.03	Phytol
19	17.684	474,634	0.22	Methyl stearate
20	17.816	355,059	0.16	Estra-1,3,5(10)-trien-17-one, 3-hydroxy-2-methoxy-
21	18.291	528,969	0.24	1-Docosene
22	18.473	370,692	0.17	Phenol, 2-methoxy-4-(1-propenyl)-
23	18.902	661,811	0.31	1,1′-Biphenyl, 4,2′,3′,4′-tetramethoxy-6-methyl-
24	19.207	302,975	0.14	Octadecanal
25	19.509	274,384	0.13	1-Cyclohexyldimethylsilyloxy-3,5-dimethylbenzene
26	19.739	1,051,485	0.49	4,8,12,16-Tetramethylheptadecan-4-olide
27	21.484	2,939,673	1.36	Methanone, [4-methyl-6-(4-dimethylamino)-1,5,2-dioxazin
28	21.808	2,679,667	1.24	1,2-benzenedicarboxylic acid
29	23.522	1,083,956	0.50	Phenol, 2-methoxy-4-(1-propenyl)-
30	27.877	4,040,391	1.87	Alpha tocospiro A
31	28.323	5,580,094	2.58	Alpha tocospiro B
32	29.044	1,692,412	0.78	CB-86
33	29.789	750,237	0.35	Phytol, acetate
34	29.972	433,449	0.20	1,1′:3′,1′′-Tercyclopentane, 2′-dodecyl-
35	32.181	486,250	0.22	Celidoniol, deoxy-
36	32.630	623,235	0.29	Vitamin E
37	36.489	5,864,204	2.71	Gamma-sitosterol
38	37.372	3,354,186	1.55	Beta-amyrin
39	38.684	12,359,743	5.72	Lupeol

Table 3
Chemical composition of the *Pimenta dioica* leaf extract obtained using Liquid chromatography-mass spectrometry analysis.

S. N.	Molecular weight	Compounds	Molecular formula
1	161.9639	2,4-Dichlorophenol	$C_6H_4Cl_2O$
2	161.9639	2,5-Dichlorophenol	$C_6H_4Cl_2O$
3	161.9639	2,6-Dichlorophenol	$C_6H_4Cl_2O$
4	161.9639	3,4-Dichlorophenol	$C_6H_4Cl_2O$
5	156.0092	(R)-2,3-Dihydroxypropane-1-sulfonate	$C_3H_8O_5S$
6	174.0429	Quinoxaline-2-carboxylic acid	$C_9H_6N_2O_2$
7	293.1739	CAY10398	$C15H_{23}N_3O_3$
8	293.1739	Lysyl-Phenylalanine	$C15H_{23}N_3O_3$
9	293.1739	Phenylalanyl-Lysine	$C15H_{23}N_3O_3$
10	304.0460	Thymidine 3,5-cyclic monophosphate	$C_{10}H_{13}N_2O_7P$
11	411.1430	Val-Trp-OH	$C_{21}H_{21}N_3O_6$
12	411.1430	Trp-Abu-OH	$C_{21}H_{21}N_3O_6$
13	411.1417	Altanserin	$C_{22}H_{22}FN_3O_2S$
14	389.1661	Diphemanil Methylsulfate	$C_{21}H_{27}NO_4S$
15	391.1777	Hexylglutathione	$C_{16}H_{29}N_3O_6S$
16	391.1784	Flavoxate	$C_{24}H_{25}NO_4$
17	414.1679	Laxiflorin	$C_{23}H_{26}O_7$
18	414.1679	Heteroflavanone C	$C_{23}H_{26}O_7$
19	414.1679	Neoisostegane	$C_{23}H_{26}O_7$
20	414.1679	Garcinone C	$C_{23}H_{26}O_7$
21	414.1679	1-(2H-1,3-Benzodioxol-5-yl)-2-[2,6-dimethoxy-4-(prop-2-en-1-yl)phenoxy]propyl acetate	$C_{23}H_{26}O_7$
22	414.1638	1,5-Dideoxy-3-C-({[2-(?-glutamylamino)-5-hydroxybenzyl]oxy}carbonyl)pentitol	$C_{18}H_{26}N_2O_9$
23	392.1835	Viguiestenin	$C_{21}H_{28}O_7$
24	392.1835	Picrasin G	$C_{21}H_{28}O_7$
25	392.1835	Lecocarpinolide J	$C_{21}H_{28}O_7$
26	415.1743	HoPhe-Lys-OH	$C_{21}H_{25}N_3O_6$
27	415.1743	Lys-HoPhe-OH	$C_{21}H_{25}N_3O_6$
28	430.1740	TyrMe-Leu-OH	$C_{22}H_{26}N_2O_7$
29	430.1740	TyrMe-Ile-OH	$C_{22}H_{26}N_2O_7$
30	408.1921	Silafluofen	$C_{25}H_{29}FO_2Si$
31	422.2026	Blasticidin S	$C_{17}H_{26}N_8O_5$
32	445.1866	PC(6:2(2E,4E)/6:2(2E,4E))	$C_{20}H_{32}NO_8P$
33	445.1866	TyrMe-Lys-OH	$C_{22}H_{27}N_3O_7$
34	462.1890	13-Hydroxy-5′-O-methylmelledonal	$C_{24}H_{30}O_9$
35	462.1890	Retrocalamin	$C_{24}H_{30}O_9$
36	462.1890	1-(3,4-Dihydroxyphenyl)-7-(4-hydroxyphenyl)-5-oxo-3-heptanyl ?-D-xylopyranoside	$C_{24}H_{30}O_9$
37	440.2100	Hydroxydiphenoxylic acid(HDPA)	$C_{28}H_{28}N_2O_3$
38	440.2046	10-Deacetyl-2-debenzoylbaccatin III	$C_{22}H_{32}O_9$
39	440.2046	3′-Hydroxy-HT2 toxin	$C_{22}H_{32}O_9$
40	441.2128	PS(12:0/0:0)	$C_{18}H_{36}NO_9P$
41	441.2165	Vilazodone	$C_{26}H_{27}N_5O_2$
42	454.2104	beta-Funaltrexamine	$C_{25}H_{30}N_2O_6$
43	473.1533	Proteacin	$C_{20}H_{27}NO_{12}$
44	473.1533	Dhurrin 6′-glucoside	$C_{20}H_{27}NO_{12}$
45	517.1074	Talampicillin hydrochloride	$C_{24}H_{24}ClN_3O_6S$
46	662.1847	Vitexin 3′'',4′''-Di-O-acetyl 2′'-O-rhamnoside	$C_{31}H_{34}O_{16}$
47	662.1847	Kaempferol 3-(2′',3′'-diacetylrhamnoside)-7-rhamnoside	$C_{31}H_{34}O_{16}$
48	640.2003	Plantamajoside	$C_{29}H_{36}O_{16}$
49	640.2003	Suspensaside	$C_{29}H_{36}O_{16}$
50	640.2003	beta-Hydroxyacteoside	$C_{29}H_{36}O_{16}$
51	640.2057	Citbismine A	$C_{35}H_{32}N_2O_{10}$
52	741.1983	3′-Deoxystreptomycin 3′α,6-bisphosphate	$C_{21}H_{41}N_7O_{18}P_2$
53	758.2633	Aldosecologanin; Dimethyl (2S,3R,4S,2′S,3′R,4′R)-4,4′-[(2Z)-4-oxo-2-butene-1,3-diyl]bis[2-(?-D-glucopyranosyloxy)-3-vinyl-3,4-dihydro-2H-pyran-5-carboxylate]	$C_{34}H_{46}O_{19}$
54	760.2862	Galα1-3Galβ1-4[Fucα1-3]GlcNAcβ-Sp	$C_{28}H_{48}N_4O_20$
55	760.2862	GalNAcα(1–3)[Fucα(1–2)]Galβ(1–4)Glcβ-Sp	$C_{28}H_{48}N_4O_20$
56	760.2862	Galα(1–3)[Fucα(1–2)]Galβ(1–4)GlcNAcβ-Sp	$C_{28}H_{48}N_4O_20$
57	760.2884	Kuwanone H	$C_{45}H_{44}O_{11}$
58	760.2862	Gala1-3[Fuca1-2]Galb1-3GlcNAcb-Sp	$C_{28}H_{48}N_4O_20$
59	742.3650	Hordatine B glucoside	$C_{35}H_{50}N_8O_{10}$
60	868.1487	Theaflavin digallate	$C_{43}H_{32}O_20$
61	861.1571	(Methylenecyclopropyl)acetyl-CoA	$C_{27}H_{42}N_7O17P3S$
62	888.2324	Cyanidin 3-[6-(6-p-coumarylglucosyl)-2-xylosylgalactoside]	$C_{41}H_{44}O_{22}$
63	888.2324	Cyanidin 3-(6′'-(E)-p-coumarylsambubioside)-5-glucoside	$C_{41}H_{44}O_{22}$
64	888.2324	Cyanidin 3-(6′'-(Z)-p-coumarylsambubioside)-5-glucoside	$C_{41}H_{44}O_{22}$
65	888.2324	Kaempferol 3-apioside-7-rhamnosyl-(1-greater than6)-(2′'-(E)-caffeoylglactoside)	$C_{41}H_{44}O_{22}$
66	917.2197	2,4-Decadienoyl-CoA	$C_{31}H_{50}N_7O_{17}P_3S$
67	917.2197	Trans-2-Methyl-5-isopropylhexa-2,5-dienoyl-CoA	$C_{31}H_{50}N_7O_{17}P_3S$
68	917.2197	Cis-2-Methyl-5-isopropylhexa-2,5-dienoyl-CoA	$C_{31}H_{50}N_7O_{17}P_3S$
69	917.2197	Geranoyl-CoA	$C_{31}H_{50}N_7O_{17}P_3S$
70	917.2197	Trans-Geranyl-CoA	$C_{31}H_{50}N_7O_{17}P_3S$

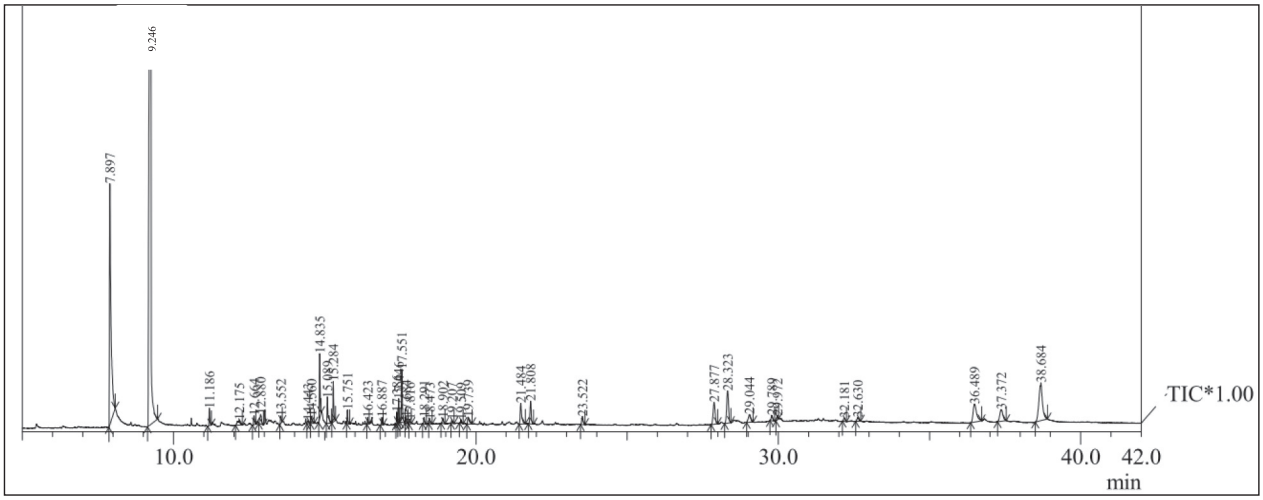

Fig. 3. The gas chromatography–mass spectrometry analysis of methanol leaf extract of *Pimenta dioica*.

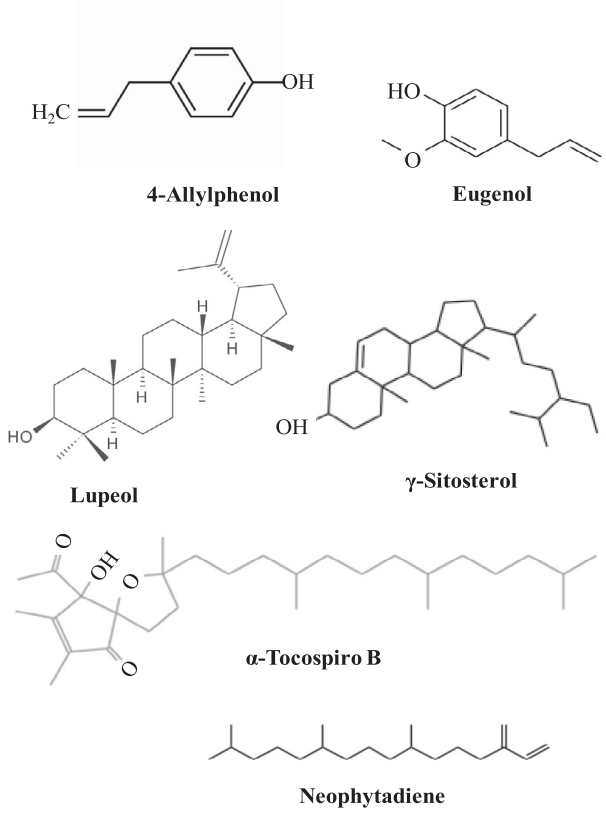

Fig. 4. Chemical structures of six major constituents in leaf extract of *P. dioica* reported through Gas chromatography–mass spectrometry analysis.

scope images of *Salvia spinosa* derived AgNPs were oval and spherical in shape (Pirtarighat et al., 2019). Jebril et al. (2020) mentioned that the *Melia azedarach* mediated silver nanoparticles were in the range of 23 nm and spherical shape. The FE-SEM images revealed the presence of spherical or nearly spherical shaped AgNPs of *Teucrium polium* leaf-derived AgNPs within the range of 70 to 100 nm (Hashemi et al., 2020). Similarly monodispersed and spherical-shaped AgNPs were observed in *Ziziphora clinopodioides* plant extract and size in between 20 and 45 nm (Esmaeili et al., 2020). Gomathi et al. (2020) also reported spherical shape of AgNPs from *Tamarindus indica* with an approximate size of 20–52 nm. SPR band at 3.3 KeV in EDX spectrum of Pd@AgNPs was reported which proved the silver nature of nanoparticles. Generally, AgNPs display absorption peaks in between 2.7 and 3.4 KeV due to SPR (Vasyliev et al., 2020). A strong peak at 3 KeV in *Cullen corylifolium* seed extract-derived AgNPs were reported by Saini et al. (2019) which proved silver metal. *Tamarindus indica* derived nanoparticles also exhibited a strong signal at 3 KeV which confirmed silver element (Gomathi et al., 2020). Monodispersed and spot type pattern of Pd@AgNPs was observed by SAED analysis. Polycrystalline and monodispersed AgNPs were reported from *Cullen corylifolium* seed extract as depicted by SAED analysis (Saini et al., 2019). Zeta potential of Pd@AgNPs was high negative which depicted its stable nature. The zeta potential of *Aesculus hippocastanum* synthesized silver nanoparticles was very negative −29.1 mV depicted its very stable nature (Küp et al., 2020). *Phyla dulcis* plant extract mediated AgNPs were very stable due to high negative value (−20 and −24 mV) in the zeta analyzer (Carson et al., 2020). FT-IR analysis showed the existence of different compounds such carboxylic acids, water, alcohols, carboxylic acids, esters, ethers, 1°, 2° amines, amides and phenol. FT-IR analysis of plants extract reported the presence of several constituents such as alcohol, phenol, aromatic and aliphatic compounds which might be responsible for bio-reduction and capping of AgNPs (Kumar et al., 2020). *Achillea millefolium* plant extract was analyzed through FT-IR at the time of AgNPs synthesis and reported the presence of following compounds alcohol, polyphenols, proteins and carboxylic acids which are involved in AgNPs formation (Yousaf et al., 2020). Flavonoids, enzymes and tannic acid available in plant extract are accountable for functionalization and capping of AgNPs (Lopes et al., 2018). GC–MS and LC-MS analysis of *Pimenta dioica* leaf extract revealed the existence of various compounds that might be accountable for the fabrication of AgNPs and larvicidal behavior of leaf extract. Methanolic extract of *Hybanthus enneaspermus* reported 39 compounds through GC–MS analysis reported activities such as anti-inflammatory, anti-microbial, hepatoprotective, parasite inhibitor and anticancer (Suman et al., 2016). GC–MS analysis of *Ammannia baccifera* aerial extract have 34 compounds major of them pyrogallol, n-hexadecanoic acid and guansoine which possess medicinal activities (Suman et al., 2013). Trans-cinnamic acid, hydroxy-L-proline, violaxanthin, deacylgymnemic acid, methyl laurate, 5, 7-

Table 4
LC_{50}, LC_{90}, regression and Chi-square analysis for the larvicidal activity of *Pimenta dioica* leaf derived silver nanoparticles and leaf extract prepared in different solvents against the 3rd instar larvae of *Aedes aegypti, Anopheles stephensi* and *Culex quinquefasciatus*.

Larvae	Extracts	Time	Regression equations	X^2 (d.f.) [a]	LC_{50}^{b}(LCL[c] and UCL[d]) ppm	LC_{90} [e] (LCL and UCL) ppm
Aedes aegypti	Methanol	24 h	$y = -3.515 + 0.038x$	5.563(5)	91.727(80.476–106.488)	125.174(109.497–160.846)
		48 h	$y = -2.540 + 0.032x$	3.736(5)	79.748(67.476–94.518)	119.989(103.012–155.011)
		72 h	$y = -2.038 + 0.031x$	3.848(5)	65.327(52.813–78.798)	106.398(90.367–137.700)
	Hexane	24 h	$y = -1.954 + 0.038x$	1.221(5)	65.631(53.777–78.062)	102.528(88.008–130.496)
		48 h	$y = -1.379 + 0.067x$	1.695(5)	51.684(40.014–63.195)	85.583(72.297–111.114)
		72 h	$y = -1.532 + 0.045x$	2.412(5)	34.118(22.458–44.614)	62.657(50.888–87.525)
	Chloroform	24 h	$y = -3.324 + 0.053x$	13.854(5)	62.272(26.681–124.285)	86.283(65.719–352.388)
		48 h	$y = -2.880 + 0.051x$	5.962(5)	56.781(47.054–67.388)	82.046(70.677–105.244)
		72 h	$y = -2.202 + 0.045x$	4.111(5)	49.207(38.700–60.102)	77.841(65.721–102.198)
	Acetone	24 h	$y = -2.874 + 0.041x$	6.663(5)	70.670(59.912–82.536)	102.184(88.919–127.836)
		48 h	$y = -2.025 + 0.037x$	3.203(5)	55.280(43.633–67.146)	90.263(76.499–116.749)
		72 h	$y = -1.755 + 0.044x$	2.457(5)	39.855(28.656–50.545)	68.953(56.931–93.728)
	Petroleum ether	24 h	$y = -3.233 + 0.031x$	8.229(5)	105.335(81.650–223.643)	147.087(114.700–503.400)
		48 h	$y = -2.342 + 0.025x$	4.152(5)	92.958(78.286–116.010)	143.834(119.526–203.124)
		72 h	$y = -2.267 + 0.031x$	3.046(5)	73.698(61.186–88.057)	115.368(98.446–149.718)
	AgNPs	24 h	$y = -1.040 + 0.032x$	4.659(5)	7.080(4.194–9.819)	15.808(12.472–22.914)
		48 h	$y = -0.856 + 0.058x$	6.459(5)	3.928(2.227–6.823)	9.812(7.339–16.345)
		72 h	$y = -1.347 + 0.155\ x$	3.830(5)	2.605(1.225–3.819)	5.084(3.859–8.737)
Culex quinquefasciatus	Methanol	24 h	$y = -1.475 + 0.046x$	1.130(5)	150.940(112.704–481.525)	239.299(164.827–974.323)
		48 h	$y = -1.564 + 0.017x$	1.896(5)	92.887(73.212–131.252)	169.002(130.833–290.243)
		72 h	$y = -1.716 + 0.083x$	3.646(5)	43.840(30.086–56.013)	83.125(68.666–111.601)
	Hexane	24 h	$y = -3.396 + 0.083x$	2.620(5)	41.128(33.136–50.283)	56.650(48.152–78.639)
		48 h	$y = -2.543 + 0.075x$	0.803(5)	33.742(25.109–42.708)	50.745(41.985–73.023)
		72 h	$y = -1.974 + 0.075x$	0.796(5)	24.246(17.148–34.881)	43.285(34.698–65.053)
	Chloroform	24 h	$y = -2.434 + 0.070x$	2.390(5)	34.700(25.323–43.313)	52.969(44.172–72.409)
		48 h	$y = -3.021 + 0.108x$	0.018(5)	27.968(20.213–35.788)	39.832(32.902–59.795)
		72 h	$y = -2.174 + 0.090x$	0.321(5)	26.245(15.633–32.367)	38.537(30.844–59.511)
	Acetone	24 h	$y = -3.561 + 0.047x$	1.257(5)	75.478(65.265–86.282)	102.641(90.819–126.623)
		48 h	$y = -2.520 + 0.039x$	3.500(5)	65.046(53.959–76.891)	98.127(84.632–124.179)
		72 h	$y = -2.096 + 0.039x$	3.765(5)	53.223(42.022–64.697)	85.768(72.658–111.191)
	Petroleum ether	24 h	$y = -2.322 + 0.032x$	3.836(5)	72.485(60.031–85.802)	112.484(96.802–142.710)
		48 h	$y = -2.880 + 0.051x$	5.962(5)	56.781(47.054–67.388)	82.046(70.677–105.244)
		72 h	$y = -2.419 + 0.058x$	2.398(5)	41.424(32.057–51.267)	63.372(53.084–85.903)
	AgNPs	24 h	$y = -1.133 + 0.21x$	3.609(5)	12.454(8.667–16.858)	26.539(20.879–40.153)
		48 h	$y = -0.982 + 0.024x$	4.831(5)	8.919(5.357–12.232)	20.562(16.309–29.750)
		72 h	$y = -0.735 + 0.032x$	7.645(5)	5.373(1.804–8.142)	14.738(11.328–22.456)
Anophele stephensi	Methanol	24 h	$y = 1.411 + 0.042x$	4.271(5)	33.851(21.548–44.731)	64.605(52.218–90.857)
		48 h	$y = -1.444 + 0.048x$	2.895(5)	30.169(18.572–40.373)	56.940(45.636–81.744)
		72 h	$y = -1.230 + 0.065x$	5.948(5)	18.859(7.579–27.611)	38.509(29.388–60.869)
	Hexane	24 h	$y = -1.147 + 0.041x$	5.134(5)	28.066(14.192–38.952)	59.424(47.089–86.100)
		48 h	$y = -0.938 + 0.046x$	7.276(5)	20.311(5.514–30.624)	48.054(36.771–73.596)
		72 h	$y = -1.267 + 0.083x$	7.214(5)	15.201(5.098–23.041)	30.578(22.787–49.053)
	Chloroform	24 h	$y = -1.868 + 0.059x$	3.762(5)	31.774(22.029–41.456)	53.575(43.397–77.493)
		48 h	$y = -1.641 + 0.058x$	3.722(5)	28.095(17.875–37.620)	50.030(39.936–74.086)
		72 h	$y = -1.379 + 0.067x$	4.003(5)	20.729(10.106–29.479)	39.992(30.919–62.333)
	Acetone	24 h	$y = -2.713 + 0.090x$	0.106(5)	30.000(21.698–38.299)	44.171(36.428–65.494)
		48 h	$y = -1.919 + 0.086x$	0.750(5)	22.435(13.517–30.564)	37.418(29.556–58.164)
		72 h	$y = -1.398 + 0.082x$	4.330(5)	17.026(7.171–24.967)	32.632(24.740–51.985)
	Petroleum ether	24 h	$y = -3.542 + 0.047x$	2.880(5)	75.915(65.515–86.605)	103.386(91.629–126.802)
		48 h	$y = -2.583 + 0.036x$	3.390(5)	71.548(59.993–84.004)	107.044(92.719–134.594)
		72 h	$y = -2.722 + 0.046x$	3.774(5)	58.999(48.783–69.870)	86.773(74.830–110.284)
	AgNPs	24 h	$y = -1.017 + 0.028x$	3.786(5)	7.618(4.489–10.484)	17.221(13.694–24.413)
		48 h	$y = -1.194 + 0.060x$	3.278(5)	4.975(2.937–7.863)	10.316(7.931–16.211)
		72 h	$y = -0.926 + 0.079x$	6.049(5)	3.269(1.158–5.079)	7.790(5.782–13.321)

Control, Zero percent mortality (1 mM silver nitrate, respective solvents and distilled water), [a]Degree of freedom, [b]lethal concentration that kills 50% of the exposed larvae; [c]95% lower confidence limit, [d] 95% upper confidence limit. [e]lethal concentration that kills 90% of the exposed larvae; $\chi 2$ = chi square, ($\alpha = 0.05$). Bold letter (LC_{50} and LC_{90})-maximum larvicidal activity at minimum concentration.

dihydroxy-4-methyl coumarin, palmatine chloride, deacylgymnemic acid, palmitoyl acetate and pterosin have been reported in *Pteridium aquilinum* leaf extract through LC-MS analysis (Panneerselvam et al., 2016). Kumar et al. (2018b) mentioned the presence of hydroxyl and carbonyl groups which are accountable for formation and capping of AgNPs which was confirmed by LC-Ms and FT-IR analysis. From the above finding it can be inferred that *P. dioica* leaf extract has different constituents which play key role for stable synthesis of silver nanoparticles.

4.2. Larvicdal activity of Pimenta dioica fabricated silver nanoparticles and leaf extract

In this research work, larvicidal activity of Pd@AgNPs and leaf extracted prepared in different solvents were examined towards the larvae of malaria, filaria and dengue vectors. Both AgNPs and solvent derived *Pimenta dioica* leaf extract exhibited comparable larvicidal activity against *An. stephensi, Cx. quinquefasciatus* and *Ae. aegypti* larvae with high parentage high percentage of mortality

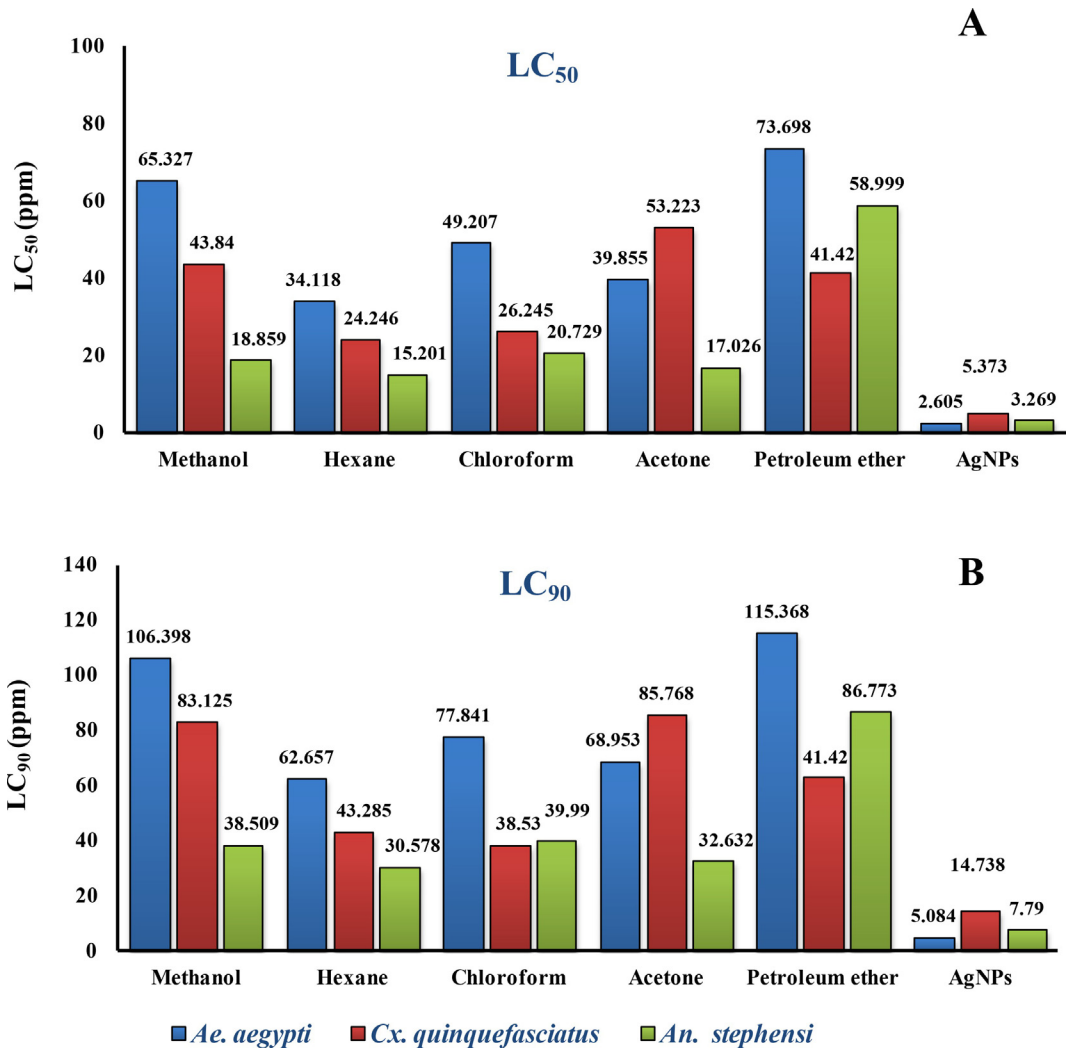

Fig. 5. (A & B)Toxicity (LC_{50} and LC_{90}) of *Pimenta dioica* leaf extracts in different solvents and silver nanoparticles against the 3rd instar larvae of *Ae. aegypti, Cx. quinquefasciatus* and *An. stephensi* mosquito vector after 72 hr of treatments.

over the control experiments. In our study, AgNPs showed strong toxicity towards *An. stephensi, Cx. quinquefasciatus* and *Ae. aegypti* larvae with minimal LC_{50}/LC_{90} value as compared to different solvents derived leaf extract. Likewise, Vimala et al. (2020) observed that AgNPs prepared using *Mimusops elengi* seed extract showed potential bio-efficacy against *Ae. aegypti* and *Cx. quinquefasciatus* larvae having LC_{50} and LC_{90} values 16.59, 18.75, 30.46 and 33.60 μg/ml, respectively. Similar to this, moderate LC_{50} and LC_{90} values were 18.9, 17.76, 12.395, 40.18, 30.82 and 36.34 ppm reported in case of *Atropa acuminate* derived AgNPs towards *Cx. quinquefasciatus, An. stephensi* and *Ae. aegypti,* respectively, after 72 hr of treatment (Rajput et al., 2020). *Rhazya stricta* extract mediated AgNPs exhibited acute toxicity against the larvae of malaria (10.57 μg/ml), filaria (11.89 μg/ml) and dengue (12.78 μg/ml) vector (Alshehri et al., 2020). Hexane, chloroform, methanol, acetone and petroleum ether leaf extract of *Pimenta dioica* showed moderate to lowest activity towards *An. stephensi*, *Cx quinquefasciatus* and *Ae. aegypti* with LC_{50} and LC_{90} value ranging in between 15.201 and 115.36 ppm after 72 hr of treatments over the control experiments whereas no mortality was observed. Likewise, Sogan et al. (2018), while working on methanol seed extracts of *Ricinus communis* reported moderate larvicidal activity against *Ae. aegypti* (LC_{50}:15.52; LC_{90}:45.24 ppm) and *An. culicifacies* (LC_{50}:9.37; LC_{90}:31.1 ppm) after 24 hr of exposure. A significant larvicidal activity of hexane followed by methanol extract of *Leucaena leucocephala* was reported against *Ae. aegypti* having LC_{50} and LC_{90} value were 0.305%, 1.025%, 0.579% and 1.619%, respectively, after 24 hr treatment. Among all solvents tried, minimum LC_{50} and LC_{90} values 111.83, 93.59, 202.77 and 163.69 ppm were observed in case of leaf extracts of *Delonix elata* towards *Ae. aegypti* and *An. stephensi*, respectively, after 24 hr of exposure (Marimuthu et al., 2012). Non-toxic nature of *Pimenta dioica* fabricated nanoparticles to *Mesocyclops thermocyclopoides* was observed when organism exposed to its $LC_{50/90}$ concentrations obtained through the larvae of mosquito vector. The non-toxic behavior of AgNPs was observed towards *Mesocyclops thermocyclopoides* by various authors (Rajput et al., 2020). AgNPs synthesized using *Pergularia daemia* and *Pergularia rubra* did not have any toxic effects towards *Poecilia reticulata*, exposed to LC_{50} and LC_{90} values of *An. stephensi* and *Ae. aegypti* for 48 hr (Patil et al., 2012a,b). Lethal concentrations estimated on the larvae of *An. stephensi* and *Cx. quinquefasciatus* of *Solanum nigrum* extract synthesized AgNPs were non-toxic towards the mosquito predators, *Diplonychus annulatum* and *Chironomus circumdatus* (Rawani et al., 2013). From the above finding it can be concluded that AgNPs of *P. dioica* showed strong larvicidal activity with minimal LC values as compared to other prepared solvents

and addition to this non-toxic against non-targeted aquatic organism *Mesocyclops thermocyclopoides* after 72 hr treatment. Several studies have been conducted on larvicidal behavior of AgNPs but exact mechanism behind the larvicidal properties is still mystery for the research. It is assumed that due to nano-size nanoparticles without difficulty insect into gut wall and interacts with sulfur and phosphorus constituents of RNA and DNA which leads to cell interference normal processes like replication, translation and proteins resulting in ultimate cell death (Kumar et al., 2020). Shahzad and Manzoor (2021) observed that AgNPs induce some morphological changes such as cellular disorganization, thickening of epidermis, disintegration of muscle layers, necrosis, and disintegration of endo and absorption of wax layer. Severe lesions such as rupture of cells, vacuolization of cell, and destruction of epithelial cells were observed in *Ae. albopictus* larvae exposed to AgNPs (Ga'al et al., 2018). Kalimuthu et al. (2017), reported similar findings, contraction of intracellular space, degeneration of nuclei and swelling in midgut were also reported in *A. aegypti* treated with *Hedychium coronarium* medicated silver nanoparticles. AgNPs also induce double-strand break in DNA through the gamma H2AX gene which are directly linked to production of ROS and apoptosis (Mao et al., 2018). Thus, the current work implicated that the plant mediated silver nanoparticles have strong mosquitocidal potential against at minimal dozes and can be considered as best alternative for mosquito control.

5. Conclusion

Nanoparticles synthesized by adding leaf extract of *P. dioica* into silver nitrate solution, colour change was observed indicating AgNPs synthesis. AgNPs showed strong absorption peaks at 422 nm. XRD and SAED patterns showed that the AgNPs crystalline in nature. SEM and TEM analysis showed spherical and triangular in shape. GC–MS and LC-MS revealed the existence of phenols (eugenol, 4-allylphenol, 2, 4-di-*tert*-butylphenol, theaflavin digallate and plantamajoside) and flavonoids (flavoxate, kaempferol and vitexin) compounds which might be play a key role for reduction, capping and stable nanoparticles synthesis. AgNPs exhibited strong larvicidal activity towards *Ae. aegypti*. *An. stephensi* and *Cx. quinquefasciatus* mosquito vectors without affecting non-targeted organism, after 72 hr of exposure. The current work demonstrated a cost-effective, scalable and green route of stable AgNPs synthesis employing *P. dioica* leaves was highly effective against mosquito vectors. Further, focusing on managing the stability, morphology, size and purification of nanoparticles from such biological entities are vital parameters this will be helpful in the development of effective nanoformulations against different mosquito vectors through the green synthesis approach. Such approach will also reduce the harmful effect of chemical based mosquitocide in both the environment and human health.

Declaration of Competing Interest

The authors declare that they have no known competing financial interests or personal relationships that could have appeared to influence the work reported in this paper.

Acknowledgements

The authors grateful to Director ICMR-National Institute of malaria Research, Dwarka Sector 8, and New Delhi for providing necessary infrastructure and support during the research work of this study. Dinesh Kumar is indebted to Indian Council of Medical Research for awarding Post-Doctoral Research Fellowship.

Funding

The research work in this publication was supported by ICMR, New Delhi through project no 3/1/3/PDF (20)/2019-HRD.

Ethics approval

This study complied with the ethical standards.

Consent to participate

Informed consent has been taken from all co-authors.

Consent for publication

The explained research work has not been published elsewhere and is not under consideration by another journal. It has been approved by all co-authors for the publication in this Journal.

References

Abbott, W.S., 1925. A method of computing the effectiveness of insecticides. J. Econ. Entomol. 18, 265–267.
Alshehri, M.A., Alanazi, N.A., Panneerselvam, C., Trivedi, S., Maggi, F., Sut, S., Dall'Acqua, S., 2020. Phytochemical analysis of Rhazya stricta extract and its use in fabrication of silver nanoparticles effective against mosquito vectors and microbial pathogens. Sci. Total Environ. 15, 700–134443.
Amarasinghe, L.D., Wickramarachchi, P.A.S.R., Aberathna, A.A.A.U., Sithara, W.S., De Silva, C.R., 2020. Comparative study on larvicidal activity of green synthesized silver nanoparticles and *Annona glabra* (Annonaceae) aqueous extract to control *Aedes aegypti* and *Aedes albopictus* (Diptera: Culicidae). Heliyon. 6 (6), e04322. https://doi.org/10.1016/j.heliyon.2020.e04322.
Benelli, G., Beier, J.C., 2017. Current vector control challenges in the fight against malaria. Acta Trop. 174, 91–96.
Bharati, M., Saha, D., 2018. Multiple insecticide resistance mechanisms in primary dengue vector, *Aedes aegypti* (Linn.) from dengue endemic districts of sub-Himalayan West Bengal, India. PLoS ONE 13 (9), e0203207.
Carson, L., Bandara, S., Joseph, M., Green, T., Grady, T., Osuji, G., Weerasooriya, A., Ampim, P., Woldesenbet, S., 2020. Green synthesis of silver nanoparticles with antimicrobial properties using *Phyla dulcis* plant extract. Foodborne pathogens and disease. 17 (8), 504–511.
Chung, M., Park, I., Seung-Hyun, K., Thiruvengadam, M., Rajakumar, G., 2016. Plant-mediated synthesis of silver nanoparticles: their characteristic properties and therapeutic applications. Nanoscale Res. Lett. 11, 40–54.
Covell, G., 1940. Anti-mosquito Measures with special Reference to India. Health Bull. 11.
Elumalai, K., Mahboob, S., Al-Ghanim, K.A., Al-Misned, F., Pandiyan, J., Baabu, P.M.K., Krishnappa, K., Govindarajan, M., 2020. Entomofaunal survey and larvicidal activity of greener silver nanoparticles: A perspective for novel eco-friendly mosquito control. Saudi J. Biol. Sci. 27 (11), 2917–2928.
Esmaeili, H., Cheraghi, N., Khanjari, A., Rezaeigolestani, M., Basti, A.A., Kamkar, A., Aghaee, E.M., 2020. Incorporation of nanoencapsulated garlic essential oil into edible films: A novel approach for extending shelf life of vacuum-packed sausages. Meat Sci. 166, 108135. https://doi.org/10.1016/j.meatsci.2020.108135.
Fadaka, A., Aluko, O., Awawu, S., Theledi, K., 2021. Green Synthesis of Gold Nanoparticles using *Pimenta dioica* Leaves Aqueous Extract and Their Application as Photocatalyst, Antioxidant, and Antibacterial Agents. J. Multidiscip. Appl. Nat. Sci. 1 (2), 78–88.
Féat, A., Federle, W., Kamperman, M., van der Gucht, J., 2019. Coatings preventing insect adhesion: An overview. Prog. Org. Coat. 134, 349–359.
Finney, D.J., 1971. Probit Analysis. Cambridge University Press, London, pp. 68–72.
Ga'al, H., Fouad, H., Mao, G., Tian, J., Jianchu, M., 2018. Larvicidal and pupicidal evaluation of silver nanoparticles synthesized using *Aquilaria sinensis* and *Pogostemon cablin* essential oils against dengue and zika viruses vector *Aedes albopictus* mosquito and its histopathological analysis. Artif. Cell Nanomed. Biotechnol. 46, 1171–1179.
Ghosh, S., Tiwari, S.S., Kumar, B., Srivastava, S., Sharma, A.K., Kumar, S., Bandyopadhyay, A., Julliet, S., Kumar, R., Rawat, A.K.S., 2015. Identification of potential plant extracts for anti-tick activity against acaricide resistant cattle ticks, *Rhipicephalus* (Boophilus) *Microplus* (Acari: Ixodidae). Exp. Appl. Acarol. 66 (1), 159–171.
Gomathi, A.C., Xavier Rajarathinam, S.R., Mohammed Sadiq, A., Rajeshkumar, S., 2020. Anticancer activity of silver nanoparticles synthesized using aqueous fruit shell extract of *Tamarindus indica* on MCF-7 human breast cancer cell line. J. Drug Delivery Sci. Technol. 55, 101376. https://doi.org/10.1016/j.jddst.2019.101376.

Govindan, L., Anbazhagan, S., Altemimi, A.B., Lakshminarayanan, K., Kuppan, S., Pratap-Singh, A., Kandasamy, M., 2020. Efficacy of Antimicrobial and Larvicidal Activities of Green Synthesized Silver Nanoparticles Using Leaf Extract of *Plumbago auriculata* Lam. Plants. 9 (11), 1577. https://doi.org/10.3390/plants9111577.

Hashemi, S.F., Tasharrofi, N., Saber, M.M., 2020. Green synthesis of silver nanoparticles using *Teucrium polium* leaf extract and assessment of their antitumor effects against MNK45 human gastric cancer cell line. J. Mol. Struct. 1208, 127889. https://doi.org/10.1016/j.molstruc.2020.127889.

Irshad, M.A., Nawaz, R., Rehman, M.Zia ur, Adrees, Md, Rizwan, Md, Ali, S., Ahmad, S., Tasleem, S., 2021. Synthesis, characterization and advanced sustainable applications of titanium dioxide nanoparticles: A review. Ecotoxicol. Environ. Saf. 212, 111978. https://doi.org/10.1016/j.ecoenv.2021.111978.

Islam, J., Zaman, K., Duarah, S., Raju, P.S., Chattopadhyay, P., 2017. Mosquito repellents: an insight into the chronological perspectives and novel discoveries. Acta Trop. 167, 216–230.

Ismail, M.M., Samir, R., Saber, F.R., Ahmed, S.R., Farag, M.A., 2020. Pimenta Oil as A potential treatment for *Acinetobacter Baumannii* wound infection: *In vitro* and *in vivo* bioassays in relation to its chemical composition. Antibiotics. 9 (10), 679. https://doi.org/10.3390/antibiotics9100679.

Jebril, S., Khanfir Ben Jenana, R., Dridi, C., 2020. Green synthesis of silver nanoparticles using *Melia azedarach* leaf extract and their antifungal activities: In vitro and in vivo. Mater. Chem. Phys. 248, 122898. https://doi.org/10.1016/j.matchemphys.2020.122898.

Kalimuthu, K., Panneerselvam, C., Chou, C., Tseng, L.C., Murugan, K., Tsai, K.H., Alarfaj, A.A., Higuchi, A., Canale, A., Hwang, J.S., Benelli, G., 2017. Control of dengue and Zika virus vector *Aedes aegypti* using the predatory copepod *Megacyclops formosanus*: synergy with *Hedychium coronarium*-synthesized silver nanoparticles and related histological changesin targeted mosquitoes. Process Saf. Environ. Prot. 109, 82–96.

Khader, S.Z..A., Syed Zameer Ahmed, S., Sathyan, J., Mahboob, M.R., Venkatesh, K.P., Ramesh, K., 2018. A comparative study on larvicidal potential of selected medicinal plants over green synthesized silver nano particles. Egypt J. Basic Appl. Sci. 5 (1), 54–62.

Kong, H., Jang, J., 2006. One-step fabrication of silver nanoparticles embedded polymer nanofibers by radical-mediated dispersion polymerization. Chem. Commun. 28, 3010–3012.

Kumar, D., Kumar, G., Agrawal, V., 2018a. Green synthesis of silver nanoparticles using *Holarrhena antidysenterica* (L.) Wall. bark extract and their larvicidal activity against dengue and filariasis vectors. Parasitol. Res. 117, 377–389.

Kumar, D., Kumar, G., Das, R., Agrawal, V., 2018b. Strong larvicidal potential of silver nanoparticles (AgNPs) synthesized using *Holarrhena antidysenterica* (L.) Wall. bark extract against malarial vector, *Anopheles stephensi* Liston. Process Saf. Environ. Prot. 116, 137–148.

Kumar, D., Kumar, P., Singh, H., Agrawal, V., 2020. Biocontrol of mosquito vectors through herbal-derived silver nanoparticles: prospects and challenges. Environ. Sci. Pollut. Res. 27 (21), 25987–26024.

Küp, F.Ö., Çoşkunçay, S., Duman, F., 2020. Biosynthesis of silver nanoparticles using leaf extract of *Aesculus hippocastanum* (horse chestnut): Evaluation of their antibacterial, antioxidant and drug release system activities. Mater. Sci. Eng. 107, 110207. https://doi.org/10.1016/j.msec.2019.110207.

Lopes, L.C.S., Brito, L.M., Bezerra, T.T., Gomes, K.N., Carvalho, F.A. De A., Chaves, M.H., Cantanhêde, W., 2018. Silver and gold nanoparticles from tannic acid: synthesis, characterization and evaluation of antileishmanial and cytotoxic activities. Anais da Academia Brasileira de Ciências. 90 (3), 2679–2689.

Mahendran, G., Kumari, B.R., 2016. Biological activities of silver nanoparticles from *Nothapodytes nimmoniana* (Graham) Mabb. fruit extracts. Food Sci. Human Well. 5, 207–218.

Maia, M.F., Moore, S.J., 2011. Plant-based insect repellents: a review of their efficacy, development and testing. Malar. J. 10, 1–15.

Manimegalai, T., Raguvaran, K., Kalpana, M., Maheswaran, R., 2020. Green synthesis of silver nanoparticle using *Leonotis nepetifolia* and their toxicity against vector mosquitoes of *Aedes aegypti* and *Culex quinquefasciatus* and agricultural pests of *Spodoptera litura* and *Helicoverpa armigera*. Environ. Sci. Pollut. Res. 27 (34), 43103–43116.

Mao, B.H., Chen, Z.Y., Wang, Y.J., Yan, S.J., 2018. Silver nanoparticles have lethal and sublethal adverse effects on development and longevity by inducing ROS-mediated stress responses. Sci. Rep. 8, 2445.

Marimuthu, G., Rajamohan, S., Mohan, R., Krishnamoorthy, Y., 2012. Larvicidal and ovicidal properties of leaf and seed extracts of *Delonix elata* (L.) Gamble (Family: Fabaceae) against malaria (*Anopheles stephensi* Liston) and dengue (*Aedes aegypti* Linn.) (Diptera: Culicidae) vector mosquitoes. Parasitol research. 111 (1), 65–77.

Marzouk, M.S., Moharram, F.A., Mohamed, M.A., Gamal-Eldeen, A.M., Aboutabl, E.A., 2007. Anticancer and antioxidant tannins from *Pimenta dioica* leaves. Zeitschrift für Naturforschung C. 62, 526–536.

McKerr, C., Lo, Yi-C., Edeghere, O., Bracebridge, S., Harley, D., 2015. Evaluation of the national Notifiable Diseases Surveillance System for dengue fever in Taiwan, 2010–2012. PLoS Negl Trop Dis 9 (3), e0003639. https://doi.org/10.1371/journal.pntd.000363910.1371/journal.pntd.0003639.g00110.1371/journal.pntd.0003639.g00210.1371/journal.pntd.0003639.g00310.1371/journal.pntd.0003639.g00410.1371/journal.pntd.0003639.g00510.1371/journal.pntd.0003639.t00110.1371/journal.pntd.0003639.t002.

Panneerselvam, C., Murugan, K., Roni, M., Aziz, Al.T., Suresh, U., Rajaganesh, R., Madhiyazhagan, P., Subramaniam, J., Dinesh, D., Nicoletti, M., Higuchi, A., Alarfaj, A.A., Munusamy, M.A., Kumar, S., Desneux, N., Benelli, G., 2016. Fern-synthesized nanoparticles in the fight against malaria: LC/MS analysis of *Pteridium aquilinum* leaf extract and biosynthesis of silver nanoparticles with high mosquitocidal and antiplasmodial activity. Parasitol. Res. 115 (3), 997–1013.

Patil, C.D., Borase, H.P., Patil, S.V., Salunkhe, R.B., Salunke, B.K., 2012a. Larvicidal activity of silver nanoparticles synthesized using *Pergularia daemia* plant latex against *Aedes aegypti* and *Anopheles stephensi* and nontarget fish *Poecillia reticulata*. Parasitol. Res. 111 (2), 555–562.

Patil, C.D., Patil, S.V., Borase, H.P., Salunke, B.K., Salunkhe, R.B., 2012b. Larvicidal activity of silver nanoparticles synthesized using *Plumeria rubra* plant latex against *Aedes aegypti* and *Anopheles stephensi*. Parasitol. Res. 110 (5), 1815–1822.

Pavunraj, M., Baskar, K., Arokiyaraj, S., Rajapandiyan, K., Alqarawi, A.A., Allah, E.F., 2020. Silver nanoparticles containing stearic acid isolated from *Catharanthus roseus*: Ovicidal and oviposition-deterrent activities on *Earias vittella* and ecotoxicological studies. Pestic. Biochem. Physiol. 1, 168–104640.

Petit, C., Lixon, P., Pileni, M.P., 1993. In situ synthesis of silver nanocluster in AOT reverses micelles. J. Phys. Chem. 97, 12974–12983.

Pillai, R.R., Sreelekshmi, P.B., Meera, A.P., 2021. Green synthesis: In-vitro anticancer activity of Iron oxide nanoparticles against human colorectal cancer cell lines. In: Abstracts of International Conferences and Meetings, vol. 1, pp. 9–9.

Pirtarighat, S., Ghannadnia, M., Baghshahi, S., 2019. Green synthesis of silver nanoparticles using the plant extract of *Salvia spinosa* grown in vitro and their antibacterial activity assessment. J Nanostruct Chem. 9, 1–9.

Prosposito, P., Burratti, L., Venditti, I., 2020. Silver nanoparticles as colorimetric sensors for water pollutants. Chemosensors 8 (2), 26. https://doi.org/10.3390/chemosensors8020026.

Rajakumar, G., Abdul Rahuman, A., 2011. Larvicidal activity of synthesized silver nanoparticles using *Eclipta prostrata* leaf extract against filariasis and malaria vectors. Acta Trop. 118 (3), 196–203.

Rajput, S., Kumar, D., Agrawal, V., 2020. Green synthesis of silver nanoparticles using Indian Belladonna extract and their potential antioxidant, anti-inflammatory, anticancer and larvicidal activities. Plant Cell Rep. 39 (7), 921–939.

Rangayasami, A., Kannan, K., Joshi, S., Subban, M., 2020. Bioengineered silver nanoparticles using Elytraria acaulis (L.f.) Lindau leaf extract and its biological applications. Biocatal. Agric. Biotechnol. 27, 101690. https://doi.org/10.1016/j.bcab.2020.101690.

Ranson, H., Burhani, J., Lumjuan, N., Black, W.C., 2010. Insecticide resistance in dengue vectors. Trop. IKA 1 (1).

Rawani, A., Ghosh, A., Chandra, G., 2013. Mosquito larvicidal and antimicrobial activity of synthesized nano-crystalline silver particles using leaves and green berry extract of *Solanum nigrum* L. (Solanaceae: Solanales). Acta Trop. 128 (3), 613–622.

Saini, H., Yadav, R., Kumar, D., Kumar, G., Agrawal, V., 2019. *Cullen corylifolium* (L.) Medik. seed extract, an excellent system for fabrication of silver nanoparticles and their multipotency validation against different mosquito vectors and human cervical cancer cell line. J Clust Sci. 31, 161–175.

Shahzad, Kiran, Manzoor, Farkhanda, 2021. Nanoformulations and their mode of action in insects: a review of biological interactions. Drug Chem. Toxicol. 44 (1), 1–11.

Shukla, D., Wijayapala, S., Vankar, P.S., 2018. Effective mosquito repellent from plant based formulation. Int. J. Mosq. Res. 5, 19–24.

Sogan, N., Kapoor, N., Singh, H., Kala, S., Nayak, A., Nagpal, B.N., 2018. Larvicidal activity of *Ricinus communis* extract against mosquitoes. J. Vector Borne Dis. 55 (4), 282. https://doi.org/10.4103/0972-9062.256563.

Suman, T.Y., Elumalai, D., Kaleena, P.K., Radhika, Rajasree, S.R., 2013. GC-MS analysis of bioactive components and synthesis of silver nanoparticle using *Ammannia bacciffera* aerial extract and its larvicidal activity against malaria and filariasis vectors). Indu Crops Prod. 47, 239–245.

Suman, T.Y., Rajasree, S.R., Jayaseelan, C., Mary, R.R., Gayathri, S., Aranganathan, L., Remya, R.R., 2016. GC-MS analysis of bioactive components and biosynthesis of silver nanoparticles using *Hybanthus enneaspermus* at room temperature evaluation of their stability and its larvicidal activity. Environ. Sci. Pollut. Res. 23, 2705–2714.

Vasyliev, G., Vorobyova, V., Skiba, M., Khrokalo, L., 2020. Green synthesis of silver nanoparticles using waste products (apricot and black currant pomace) aqueous extracts and their characterization. Adv. Mater. Sci. Eng. 2020, 1–11.

Vimala, G., Thilaga, M., Veni, T., Devi, K., Gopalarathinam, K., 2020. Larvicidal activity of aqueous *Mimusops elengi* seeds-synthesized silver nanoparticles against *Aedes aegypti* and *Culex quinquefasciatus*. Int. J. Mosq. Res. 7, 30–36.

Waris, Md, Nasir, S., Abbas, S., Azeem, Md., Ahmad, B., Khan, N.A., Hussain, B., Al-Ghanim, K.A., Al-Misned, F., Mulahim, N., Mahboob, S., 2020. Evaluation of larvicidal efficacy of *Ricinus communis* (Castor) and synthesized green silver nanoparticles against *Aedes aegypti* L. Saudi J. Biol. Sci. 27 (9), 2403–2409.

WHO, 1988. Instructions for determining the susceptibility or resistance of mosquito larvae to insecticides. WHO/VBC/81.807, Geneva.

Yadav, R., Saini, H., Kumar, D., Pasi, S., Agrawal, V., 2019. Bioengineering of *Piper longum* L. extract mediated silver nanoparticles and their potential biomedical applications. Mater. Sci. Eng., C 104.

Yousaf, H., Mehmood, A., Ahmad, K.S., Raffi, M., 2020. Green synthesis of silver nanoparticles and their applications as an alternative antibacterial and antioxidant agents. Mater. Sci. Eng. 112, 110901.

Zabka, M., Pavela, R., Slezakova, L., 2009. Antifungal effect of *Pimenta dioica* essential oil against dangerous pathogenic and toxinogenic fungi. Ind. Crops Prod. 30, 250–253.